

# Synthesis of Unit Hydrographs from a Digital Elevation Model

Theodore G. Cleveland, Ph.D.<sup>1</sup>; David B. Thompson, Ph.D.<sup>2</sup>; Xing Fang, Ph.D.<sup>3</sup>; and Xin He<sup>4</sup>

**Abstract:** Characterization of hydrologic processes of a watershed requires estimation of the specific time-response characteristics of the watershed. In the absence of observations these characteristics are estimated from watershed physical characteristics. An exploratory assessment of a particle-tracking approach for parametrizing unit hydrographs from topographic information for applicable Texas watersheds is presented. The study examined 126 watersheds in Texas, for which rainfall and runoff data were available with drainage areas ranging approximately from 0.65 to 388 km, main channel lengths ranging approximately from 1.1 to 80 km, and dimensionless main channel slopes ranging approximately from 0.0002 to 0.02. Unit hydrographs based on entirely on topographic information were generated and used to simulate direct runoff hydrographs from observed rainfall events. These simulated results are compared to observed results to assess method performance. Unit hydrographs were also generated by a conventional analysis (of the observed data) approach to provide additional performance comparison. The results demonstrate that the procedure is a reasonable approach to estimate unit hydrograph parameters from a relatively minimal description of watershed properties, in this case elevation and a binary development classification. The method produced unit hydrographs comparable to those determined by conventional analysis and thus is a useful synthetic hydrograph approach.

**DOI:** 10.1061/(ASCE)0733-9437(2008)134:2(212)

**CE Database subject headings:** Streamflow; Rainfall; Watershed management; Texas; Hydrographs; Digital techniques.

## Introduction

The unit hydrograph (UH) is a model to predict the streamflow hydrograph from a rainfall hyetograph at the outlet of a basin. It can be expressed as

$$q(t) = \int_0^T r(\tau)f(t-\tau)d\tau \quad (1)$$

where  $q(t)$ =unit discharge from a basin at time  $t$ ;  $r(t)$ =input function that represents either rainfall or excess rainfall;  $f(t-\tau)$ =response function (the unit hydrograph); and  $T$ =duration of the input. Eq. (1) assumes that basins respond as linear systems and this assumption is the main criticism of unit hydrograph theory. Despite this criticism, unit hydrographs are used to estimate streamflow from relatively small basins, typically for engineering purposes and often produce reasonable results. With

the linearity assumption, the response,  $f(t-\tau)$ , has the same properties as a probability density function; specifically it integrates to unity on the range  $(-\infty, \infty)$ , and  $f(t-\tau) \geq 0$  for any values of  $(t-\tau)$ .

Traditionally as suggested by Sherman (1932) and explained in many references, the UH of a watershed is derived from observed runoff and rainfall records. For ungauged watersheds, such data are unavailable, and synthetic methods are used to infer the unit hydrograph. These methods vary in how the geomorphic information from the watershed is incorporated to produce estimates of the unit hydrograph.

Clark (1945) developed a method for generating unit hydrographs for a watershed based on routing a time-area relationship through a linear reservoir. Excess rainfall covering a watershed to some unit depth is released instantly and allowed to traverse the watershed and the time-area relation represents the translation hydrograph. The time-area relationships are usually inferred from a topographic map. The linear reservoir is added to reflect storage effects of the watershed. Clark's method clearly attempts to relate geomorphic properties to watershed response.

Leinhard (1964) derived a unit hydrograph model using a statistical-mechanical analogy and two important assumptions. The first is that the travel time taken by an excess raindrop landing on the watershed to the outlet is proportional to the pathline distance the raindrop must travel. The second assumption is that the area swept by any characteristic distance is proportional to some power of that characteristic distance. Dimensionally, the ratio of the path length to travel time would be a characteristic velocity. Leinhard's derivation did not attempt to relate watershed properties that might appear on a map to the hydrologic response, but the connection was implied.

Rodriguez-Iturbe and Valdes (1979) and Gupta et al. (1980) examined the structure of unit hydrographs conceptualized as

<sup>1</sup>Associate Professor, Dept. of Civil and Environmental Engineering, Univ. of Houston, Houston, TX 77204 (corresponding author). E-mail: cleveland@uh.edu

<sup>2</sup>Director of Civil Engineering for Hydrology and Hydraulics, R.O. Anderson, Inc. E-mail: dthompson@roanderson.com

<sup>3</sup>Professor, Dept. of Civil Engineering, Lamar Univ., Beaumont, TX 77710. E-mail: xing.fang@lamar.edu

<sup>4</sup>Doctoral Candidate, Dept. of Civil and Environmental Engineering, Univ. of Houston, Houston, TX 77204. E-mail: hexinbit@hotmail.com

Note. Discussion open until September 1, 2008. Separate discussions must be submitted for individual papers. To extend the closing date by one month, a written request must be filed with the ASCE Managing Editor. The manuscript for this paper was submitted for review and possible publication on November 27, 2006; approved on April 9, 2007. This paper is part of the *Journal of Irrigation and Drainage Engineering*, Vol. 134, No. 2, April 1, 2008. ©ASCE, ISSN 0733-9437/2008/2-212-221/\$25.00.

residence time distributions from a geomorphic perspective and provided guidance to parametrize the hydrographs in terms of Horton's bifurcation ratio, stream length ratio, and stream area ratio and an independently specified basin lag time. In these works the result was called a geomorphic unit hydrograph (GUH). Like Leinhard's derivation the relationships of path, path length, and travel time are fundamental in the development of the unit hydrographs. Furthermore, all these derivations rely on the concept of representing the excess rainfall as an ensemble of particles distributed on the watershed.

Jin (1992) developed a GUH based on a gamma distribution and suggested a way to parametrize the distribution based on path types and a streamflow velocity. Like the prior work, the concept of distance, velocity, and time was crucial. In Jin's GUH the initial estimate of velocity was based on a peak observed discharge for a basin, thus some kind of streamflow record was required, or some estimate of bankflow discharge would be required.

Maidment (1993) developed a geographic information system (GIS)-based approach using the classical time-area method and GIS scripts. Muzik (1996) approached the time-area modeling in a similar fashion. These works used flow routing based on a constant velocity or subjectively predetermined velocity map independently incorporating concepts of a GUH.

Kull and Feldman (1998) assumed that travel time for each cell in the watershed was simply proportional to the time of concentration scaled by the ratio of travel length of the cell over the maximum travel length. Thus the velocity from any point to the outlet is uniform and constant. Each cell's excess rainfall is lagged to the outlet based on the travel distance from the cell. Travel time in overland and channel flow are determined beforehand. This approach is essentially a version of Clark's (1945) methodology and is implemented in HEC-GEOHMS (HEC 2000).

Saghafian and Julien (1995) derived a GIS-based time-to-equilibrium approach for any location on a watershed based on a uniform overland flow model, that incorporated elevation information. Saghafian et al. (2002) used this concept to develop a time-variable isochrone GIS technique to generate runoff hydrographs for nonuniform hydrographs (nonuniform in space and time).

Olivera and Maidment (1999) developed a raster-based, spatially distributed routing technique based on a first-passage-time response function (a gamma-type unit hydrograph at the cell scale).

Lee and Yen (1997) recognized that a kinematic-wave model could be used to estimate travel times over a path to the watershed outlet and developed a procedure to parametrize a GUH by relating slope along a set of planes defined by stream order that are linked to each other and the watershed outlet.

Additionally numerous methods in the literature relate properties such as selected lengths, slopes, fraction of sewer served areas, etc. to unit hydrograph timing parameters. A selection of the more common methods appears in Roussel et al., 2005. The methods in the Roussel report generally use a handful of measures to estimate the timing parameters and were developed prior to common availability of digital elevation data.

The significance of all these studies is that the concepts of distance, velocity, and time need to be linked to physical characteristics of the watershed to parametrize a unit hydrograph in the absence of observed runoff and rainfall data. Additionally, the GIS studies appeared to have evolved in parallel to the GUH theory incorporating similar ideas while implicitly parametrizing the underlying GUH by various methods. Shamseldin and Nash

(1998) argue that GUH theory is equivalent to the assumption of a generalized UH equation described by a distribution whose parameters must subsequently be related by regression (or otherwise) to appropriate catchment characteristics.

This paper presents the results of a hybrid approach to estimate the parameters of a GUH by analysis of an arrival time distribution of rainfall particles, whose travel speeds and paths are determined by local watershed slope. A particle-tracking program was used to generate the arrival time distribution, and 30-m digital elevation model (DEM) data were used to compute local slopes and travel paths. A UH equation was then fit to the arrival time distribution to extract a timing parameter and a shape parameter, unique to each watershed—an approach similar to Shamseldin and Nash's (1998) argument.

The study examined 126 watersheds in Texas, for which rainfall and runoff data were available. For the selected watersheds, the drainage areas range from approximately 0.65 to 388 km<sup>2</sup>, main channel lengths range from approximately 1.1 to 80 km, and dimensionless main channel slopes range from approximately 0.0002 to 0.02. Because a rainfall-runoff database exists for the study watersheds, the resulting unit hydrographs can be used to generate runoff hydrographs for the historical rainfalls and these modeled hydrographs are compared to the observed hydrographs to evaluate the performance of the particle tracking approach. UHs were also generated by a conventional analysis (of the observed data) approach to provide a performance comparison.

## Rainfall-Runoff Database

A digital database of rainfall and runoff values for over 2,600 storms from 126 developed and undeveloped watersheds in Texas was used for the research. A portion of the database is described and tabulated in Asquith et al. (2004), and an additional 33 watersheds in the Houston area supplements the Asquith database. A watershed properties database was developed from 30-m DEMs. The watershed properties database is described in Roussel et al. (2005), and it too is supplemented with properties from the 33 Houston area watersheds. Fig. 1 is a map of the study watershed locations that illustrates the spatial distribution of the study. Table 1 lists the individual stations depicted in Fig. 1, some selected physical characteristics, and the hydrograph parameters determined by the method described in this paper.

## Methodology

Generating an excess rainfall arrival time distribution at the watershed outlet was addressed by placing a computational particle on each cell of a DEM grid, computing the direction this particle would move from an eight-cell pour point model (O'Calligan and Mark 1984), and computing the velocity of the particle according to a uniform flow equation whose velocity term is determined by the slope along the particle path at the particle's current position. A short interval of time is allowed to pass, and the particle's new position is calculated and the entire computational process is repeated.

Over the short time interval, the particle will move a distance along its pathline determined by the product of the appropriate characteristic velocity and the time interval. Fig. 2 illustrates the relationship between Cartesian and path line coordinates. This work assumed the square of velocity is proportional to watershed

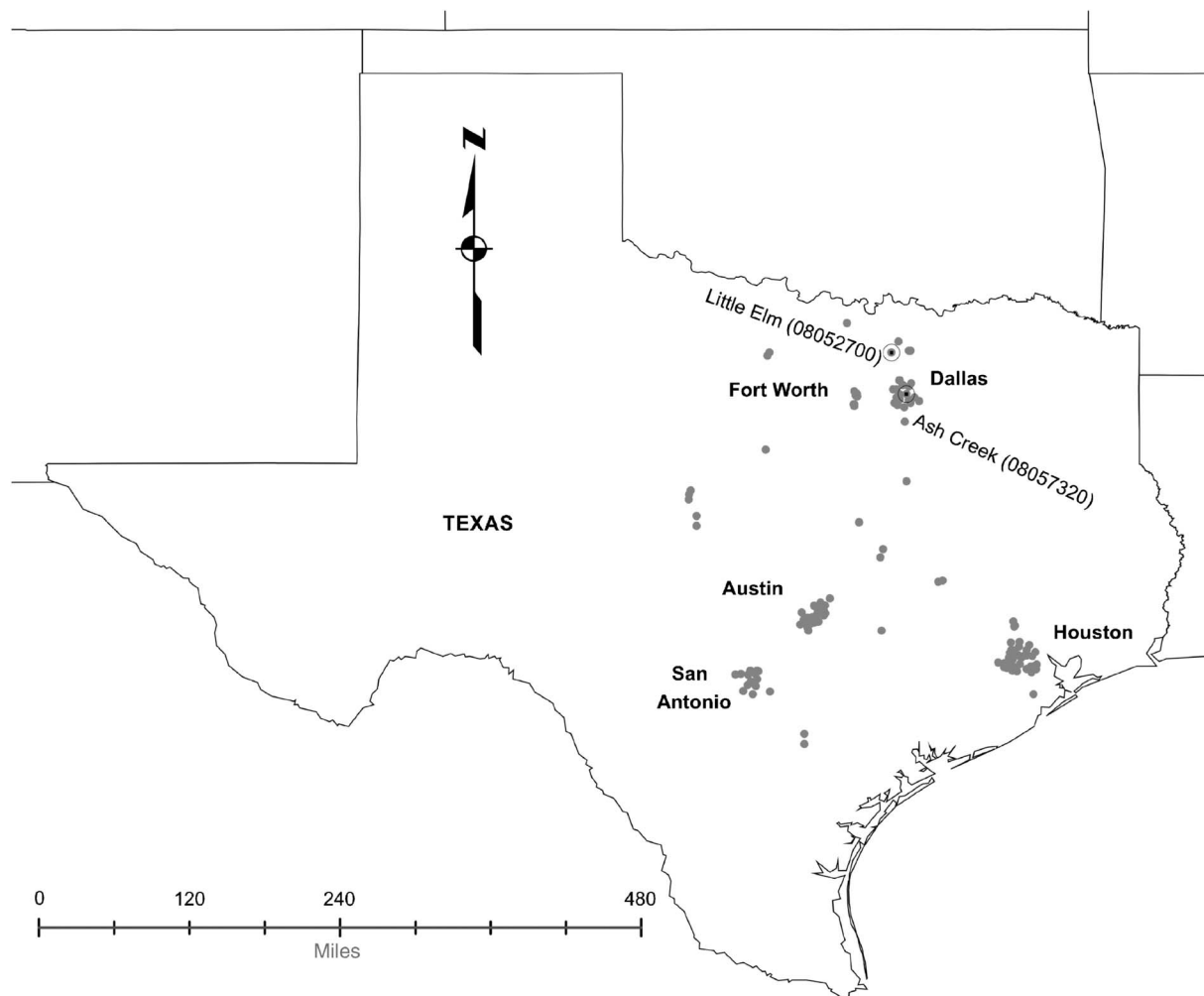


Fig. 1. Map of study watershed locations

slope at any location, and therefore the velocity field depends on the particle positions.

Eq. (2) represents the formula in a path line coordinate system used to determine the velocity at any location in the watershed

$$u(\xi)|u(\xi)| = -k^2 \frac{\partial z}{\partial \xi} \quad (2)$$

The value  $u$ =velocity of the particle along the path;  $\xi$ =distance or location on the particle's flow path;  $z$ =watershed elevation at the current particle position; and  $k^2$  represents the square of velocity of the particle on a unit slope. The absolute value formulation is used so that the numerical method preserves correct directional information (flow is always downslope). This approach is similar to existing methods, but makes no distinction between channel and overland flow. All results presented in this paper are based on this velocity model.

In the present work we have adopted the following structure for  $k$

$$k = \frac{1.5}{n_f} d^{2/3} \quad (3)$$

where  $n_f$ =frictional term (an adjustable parameter) that is conceptually analogous but not numerically equal to Manning's  $n$ ; and  $d$ =mean flow depth (an adjustable parameter). This particular structure is selected to make the procedure look like Manning's

equation, although the writers prefer the concept of unit-slope characteristic velocity. The resulting particle kinematics are analogs to Wooding's (1965) kinematic wave analysis for overland flow and similar to the isochrone derivation technique of Saghafian and Julien (1995) who adapted the kinematic wave theory for distributed rainfall-runoff modeling and presented an example (Saghafian et al. 2002) for a watershed in West Africa. The applicability of the velocity model is subject to an important consideration regarding the backwater effect from downstream. In this work we have implicitly assumed that there is no backwater effect, but the Houston watersheds are known to have backwater effects at the gauging stations as well as tidal influence. Additionally the Houston data have slopes one order of magnitude smaller than the remaining watersheds and the applicability of a kinematic-wave type flow is questionable. Thus the results with regard to Houston watersheds are anticipated to exhibit greater variability than the other watersheds in the study.

Fig. 2 displays a single path for clarity. On the illustrated watershed, using a 30-m resolution DEM, 20,639 paths were identified (one for each grid cell on the approximately 8.6 km<sup>2</sup> watershed) that drain the outlet located in the lower left corner of the figure. On some of the larger watersheds, over 500,000 paths were identified. Each path is defined by an individual particle's starting point, and each particle follows its own unique path. Eq. (3) is evaluated at least once for each path, and multiple times

**Table 1.** Locations, Physical Characteristics, and Unit Hydrograph (UH) Values for Texas Watersheds

Station number	Name	TDA	MCL	Slope	DEVF	$Q_p$	$T_p$
8068438	Swale No. 8 at Woodlands, Tex.	1.4	1.2	0.0077	0	0.341	0.41
8178640	West Elm Creek at San Antonio, Tex.	6.4	4.9	0.0204	0	0.118	2.13
8057500	Honey Creek sub. 11 near McKinney, Tex.	5.4	3.3	0.0110	0	0.113	2.25
8058000	Honey Creek sub. 12 near McKinney, Tex.	3.1	3.4	0.0103	0	0.111	2.29
8068440	Lake Harrison at drop inlet at Woodlands, Tex.	1.8	2.1	0.0062	0	0.133	1.10
8139000	Deep Creek sub. 3 near Placid, Tex.	8.1	5.4	0.0152	0	0.106	2.37
8178645	East Elm Creek at San Antonio, Tex.	6.4	6.4	0.0163	0	0.103	2.44
8050200	Elm Fork Trinity River sub. 6 near Muenster, Tex.	2.3	4.3	0.0107	0	0.104	2.43
8187000	Escondido Creek sub. 1 near Kennedy, Tex.	7.9	4.5	0.0098	0	0.101	2.52
8042650	North Creek sub. 28A near Jermyn, Tex.	17.0	7.5	0.0138	0	0.094	2.66
8181000	Leon Creek Tributary at FM 1604, San Antonio, Tex.	14.4	8.7	0.0162	0	0.093	2.67
8094000	Green Creek sub. 1 near Dublin, Tex.	6.2	5.4	0.0090	0	0.093	2.71
8158880	Boggy Creek (south) at Circle S Road, Austin, Tex.	9.3	7.1	0.0114	0	0.091	2.74
8096800	Cow Bayou sub. 4 near Bruceville, Tex.	13.1	7.2	0.0112	0	0.090	2.77
8158840	Slaughter Creek at FM 1826, Austin, Tex.	22.7	8	0.012	0	0.089	2.81
8159150	Wilbarger Creek near Pflugerville, Tex.	11.6	6.0	0.0086	0	0.089	2.82
8052630	Little Elm Creek sub. 10 near Gunter, Tex.	5.3	5.3	0.0065	0	0.086	2.92
8178600	Panther Springs Creek at FM 2696 near San Antonio, Tex.	24.9	11.4	0.0131	0	0.082	3.01
8158810	Bear Creek below FM 1826, Driftwood, Tex.	31.9	10.1	0.0113	0	0.081	3.04
8140000	Deep Creek sub. 8 near Mercury, Tex.	19.0	9.5	0.0102	0	0.081	3.06
8158100	Walnut Creek at FM 1325, Austin, Tex.	33.0	9.1	0.0098	0	0.081	3.07
8057120	McKamey Creek at Preston Road, Dallas, Tex.	17.0	8.4	0.0075	0	0.078	3.20
8181400	Helotes Creek at Helotes, Tex.	38.6	15.8	0.0133	0	0.074	3.29
8137000	Mukewater Creek sub. 9 near Trickham, Tex.	10.6	7.1	0.0052	0	0.075	3.34
8182400	Calaveras Creek sub. 6 near Elmendorf, Tex.	18.5	7.8	0.0057	0	0.074	3.37
8187900	Escondido Creek sub. 11 near Kennedy, Tex.	22.8	7.8	0.0056	0	0.074	3.37
8154700	Bull Creek at Loop 360, Austin, Tex.	59.0	16.2	0.0107	0	0.070	3.50
8077100	Clear Creek Tributary at Hall Road, Houston, Tex.	3.40	3.0	0.0015	0	0.051	3.27
8158200	Walnut Creek at Dessau Road, Austin, Tex.	68.5	17.6	0.0070	0	0.061	4.00
8158860	Slaughter Creek at FM 2304, Austin, Tex.	60.2	20.6	0.0079	0	0.060	4.05
8136900	Mukewater Creek sub. 10A near Trickham, Tex.	56.4	20.0	0.0077	0	0.060	4.04
8042700	North Creek near Jacksboro, Tex.	62.2	18.6	0.0068	0	0.060	4.08
8158825	Little Bear Creek at FM 1626, Manchaca, Tex.	54.5	20.2	0.0067	0	0.058	4.19
8158820	Bear Creek at FM 1626, Manchaca, Tex.	63.5	23.9	0.0075	0	0.057	4.27
8063200	Pin Oak Creek near Hubbard, Tex.	47.1	14.1	0.0042	0	0.057	4.29
8075780	Greens Bayou at Cutten Road near Houston, Tex.	20.9	6.9	0.0015	0	0.022	6.66
8074780	Keegans Bayou at Keegan Road near Houston, Tex.	22.4	9.4	0.0019	0	0.046	5.76
8137500	Mukewater Creek at Trickham, Tex.	179.5	31.2	0.0056	0	0.049	4.95
8068400	Panther Branch near Conroe, Tex.	67.7	14.3	0.0024	0	0.020	8.81
8098300	Little Pond Creek near Burlington, Tex.	59.6	22.1	0.0026	0	0.045	5.43
8155200	Barton Creek at SH 71, Oak Hill, Tex.	232.4	45.9	0.0050	0	0.042	5.66
8074800	Keegans Bayou at Roark Road near Houston, Tex.	32.9	13.3	0.0013	0	0.035	8.59
8158700	Onion Creek near Driftwood, Tex.	320.7	53.6	0.0045	0	0.039	6.05
8108200	North Elm Creek near Cameron, Tex.	120.2	32.1	0.0026	0	0.040	6.05
8068450	Panther Branch near Spring, Tex.	89.4	22.9	0.0018	0	0.017	10.77
8052700	Little Elm Creek near Aubrey, Tex.	189.5	37.4	0.0024	0	0.037	6.41
8075900	Greens Bayou at U.S. Hwy. 75 near Houston, Tex.	94.9	17.8	0.0010	0	0.012	14.78
8155300	Barton Creek at Loop 360, Austin, Tex.	302.3	72.6	0.0041	0	0.035	6.72
8158800	Onion Creek at Buda, Tex.	433.6	78.8	0.0039	0	0.034	6.97
8076000	Greens Bayou near Houston, Tex.	178.1	31.5	0.0009	0	0.009	17.83
8076700	Greens Bayou at Ley Road, Houston, Tex.	471.8	48.4	0.0008	0	0.007	27.92
8177600	Olmos Creek Tributary at FM 1535, Shavano Park, Tex.	0.8	2.1	0.0147	1	1.178	0.22
8048530	Sycamore Creek Tributary above Seminary South Shopping Center, Fort Worth, Tex.	2.5	2.7	0.0118	1	0.790	0.32
8074400	Lazybrook Street Storm Sewer at Houston, Tex.	0.3	1.1	0.0047	1	0.360	0.39



**Table 1.** (Continued.)

Station number	Name	TDA	MCL	Slope	DEVF	$Q_p$	$T_p$
8178690	Salado Creek Tributary at Bitters Road, San Antonio, Tex.	1.1	1.9	0.0074	1	0.653	0.40
8073630	Bettina Street Ditch at Houston, Tex.	3.6	1.2	0.0041	1	0.086	2.31
8178736	Salado Creek Tributary at Bee Street, San Antonio, Tex.	1.8	2.7	0.0094	1	0.637	0.40
8048540	Sycamore Creek Tributary at IH 35W, Fort Worth, Tex.	3.3	3.8	0.0112	1	0.596	0.43
8178300	Alazan Creek at St. Cloud Street, San Antonio, Tex.	8.5	5.8	0.0167	1	0.657	0.38
8156650	Shoal Creek at Steck Avenue, Austin, Tex.	7.0	4.8	0.0116	1	0.521	0.48
8057415	Elam Creek at Seco Boulevard, Dallas, Tex.	2.5	3	0.0072	1	0.456	0.56
8057130	Rush Branch at Arapaho Road, Dallas, Tex.	3.3	4.2	0.0091	1	0.453	0.56
8155550	West Bouldin Creek at Riverside Drive, Austin, Tex.	6.9	5.9	0.0126	1	0.492	0.51
8178620	Lorence Creek at Thousand Oaks Boulevard, San Antonio, Tex.	10.5	5.8	0.012	1	0.473	0.53
8057440	Whites Branch at IH 625, Dallas, Tex.	6.8	5.7	0.0086	1	0.349	0.72
8055580	Joes Creek at Royal Lane, Dallas, Tex.	4.9	4.8	0.0073	1	0.332	0.76
8158920	Williamson Creek at Oak Hill, Tex.	16.3	8.0	0.012	1	0.380	0.66
8157000	Waller Creek at 38th Street, Austin, Tex.	5.7	6.6	0.0098	1	0.355	0.71
8057435	Newton Creek at IH 635, Dallas, Tex.	15.3	6.6	0.0096	1	0.347	0.72
8048550	Dry Branch at Blandin Street, Fort Worth, Tex.	2.9	3.2	0.0047	1	0.285	0.90
8156700	Shoal Creek at Northwest Park, Austin, Tex.	16.5	7.3	0.0101	1	0.343	0.73
8057020	Coombs Creek at Sylvan Ave, Dallas, Tex.	11.7	8.2	0.0097	1	0.304	0.82
8156750	Shoal Creek at White Rock Drive, Austin, Tex.	17.7	8.3	0.0095	1	0.297	0.84
8158380	Little Walnut Creek at Georgian Drive Austin, Tex.	13.6	6.5	0.0074	1	0.274	0.91
8157500	Waller Creek at 23rd Street, Austin, Tex.	10.8	8.3	0.0094	1	0.292	0.85
8158400	Little Walnut Creek at IH 35, Austin, Tex.	14.8	7.2	0.0071	1	0.245	1.02
8074145	Bingle Road Storm Sewer at Houston, Tex.	0.5	1.1	0.0011	1	0.182	2.77
8057418	Fivemile Creek at Kiest Boulevard, Dallas, Tex.	20.9	9.1	0.0079	1	0.232	1.07
8073800	Bering Ditch at Woodway Drive, Houston, Tex.	7.2	2.2	0.0019	1	0.054	1.14
8057425	Woody Branch at IH 625, Dallas, Tex.	26.8	9.9	0.0083	1	0.229	1.08
8057050	Cedar Creek at Bonnieview Road, Dallas, Tex.	24.6	10	0.0079	1	0.217	1.14
8048600	Dry Branch at Fain Street, Fort Worth, Tex.	6.7	6.2	0.0048	1	0.187	1.34
8057160	Floyd Branch at Forest Lane, Dallas, Tex.	11.9	8.6	0.0064	1	0.196	1.27
8057320	Ash Creek at Highland Road, Dallas, Tex.	18.6	8.7	0.0061	1	0.186	1.34
8158050	Boggy Creek at US 183, Austin, Tex.	32.7	11.9	0.0080	1	0.194	1.27
8181450	Leon Creek Tributary at Kelly Air Force Base, Tex.	3.2	5.0	0.0032	1	0.146	1.73
8056500	Turtle Creek at Dallas, Tex.	16.5	10.2	0.0065	1	0.176	1.41
8048820	Little Fossil Creek at IH 820, Fort Worth, Tex.	14.7	9.7	0.006	1	0.169	1.47
8055600	Joes Creek at Dallas, Tex.	14.8	10.9	0.0060	1	0.158	1.56
8075300	Sims Bayou at Carlsbad Street Houston, Tex.	9.9	5.1	0.0028	1	0.046	3.95
8158930	Williamson Creek at Manchaca Road, Austin, Tex.	48.6	16.7	0.0090	1	0.171	1.43
8158500	Little Walnut Creek at Manor Road, Austin, Tex.	31.4	13.8	0.0069	1	0.153	1.60
8057140	Cottonwood Creek at Forest Lane, Dallas, Tex.	22.4	12.0	0.0059	1	0.143	1.73
8057420	Fivemile Creek at US Highway 77W, Dallas, Tex.	37.3	13.4	0.0065	1	0.146	1.68
8061620	Duck Creek at Buckingham Road, Garland, Tex.	19.9	8.9	0.0042	1	0.128	1.94
8156800	Shoal Creek at 12th Street, Austin, Tex.	33.0	17.0	0.0079	1	0.149	1.64
8075600	Berry Bayou Tributary at Globe Street, Houston, Tex.	4.1	3.6	0.0017	1	0.027	4.57
8048520	Sycamore Creek at IH 35W, Fort Worth, Tex.	45.7	12.1	0.0055	1	0.134	1.84
8075750	Hunting Bayou Tributary at Cavalcade Street, Houston, Tex.	3.1	2.9	0.0013	1	0.052	2.42
8055700	Bachman Branch at Dallas, Tex.	28.6	12.5	0.0052	1	0.124	1.99
8178555	Harlendale Creek at West Harding Street, San Antonio, Tex.	4.9	6.5	0.0024	1	0.093	2.69
8075550	Berry Bayou at Gilpin Street at Houston, Tex.	6.6	5.4	0.0018	1	0.056	2.23
8074910	Hummingbird Street Ditch at Houston, Tex.	0.8	2.3	0.0008	1	0.115	1.26
8048850	Little Fossil Creek at Mesquite Street, Fort Worth, Tex.	33.3	15.1	0.0051	1	0.105	2.32
8061920	South Mesquite Creek at SH 352, Mesquite, Tex.	33.4	12.3	0.0039	1	0.094	2.62
8057445	Prairie Creek at US Highway 175, Dallas, Tex.	23.2	13.5	0.0038	1	0.087	2.82
8074100	Cole Creek at Guhn Road at Houston, Tex.	18.3	8.1	0.0023	1	0.03	6.42
8075760	Hunting Bayou at Falls Street at Houston, Tex.	6.7	6.5	0.0016	1	0.041	5.40
8158970	Williamson Creek at Jimmy Clay Road, Austin, Tex.	71.0	28.3	0.0065	1	0.088	2.75

**Table 1.** (Continued.)

Station number	Name	TDA	MCL	Slope	DEVF	$Q_p$	$T_p$
8075700	Berry Creek at Galveston Road at Houston, Tex.	12.6	6.8	0.0016	1	0.046	3.23
8075650	Berry Bayou at Forest Oaks Street, Houston, Tex.	27.7	7.9	0.0016	1	0.023	6.69
8074750	Brays Bayou at Addicks-Clodine Road, Houston, Tex.	2.3	2.8	0.0005	1	0.026	2.46
8158600	Walnut Creek at Webberville Road, Austin, Tex.	138.9	31.4	0.0051	1	0.065	3.72
8075400	Sims Bayou at Hiram Clarke Street, Houston, Tex.	52.4	10.6	0.0017	1	0.029	8.74
8061950	South Mesquite Creek at Mercury Road, Mesquite, Tex.	60.4	20.4	0.0031	1	0.053	4.59
8074150	Cole Creek at Deihl Road, Houston, Tex.	19.4	10.7	0.0013	1	0.024	6.10
8074540	Little Whiteoak Bayou at Trimble Street, Houston, Tex.	46.7	14.5	0.0016	1	0.038	7.68
8075730	Vince Bayou at Pasadena, Tex.	21.4	8.4	0.0009	1	0.033	6.15
8075770	Hunting Bayou at IH-610, Houston, Tex.	41.7	12.5	0.0012	1	0.044	3.80
8076200	Halls Bayou at Deertrail Street at Houston, Tex.	23.3	12.4	0.0010	1	0.016	11.09
8074900	Willow Waterhole Bayou at Landsdowne Street, Houston, Tex.	29.0	12.2	0.0009	1	0.012	13.00
8074760	Brays Bayou at Alief Road, Alief, Tex.	36.5	13.8	0.0008	1	0.019	6.91
8074850	Bintliff Ditch at Bissonnet at Houston, Tex.	11.4	10.9	0.0005	1	0.021	7.44
8076500	Halls Bayou at Houston, Tex.	74.4	24.0	0.0010	1	0.010	14.46
8074500	Whiteoak Bayou at Houston, Tex.	223.7	33.1	0.0011	1	0.022	14.79
8075500	Sims Bayou at Houston, Tex.	163.3	30.3	0.0010	1	0.010	11.52
8074810	Brays Bayou at Gessner Drive, Houston, Tex.	137.9	22.6	0.0007	1	0.016	12.44
8075000	Brays Bayou at Houston, Tex.	246.0	33.8	0.0007	1	0.008	15.50

Note: TDA=total drainage area km<sup>2</sup>; MCL=main channel length km; SLOPE=dimensionless main channel slope; DEVF=basin development factor (0=undeveloped, 1=developed);  $Q_p$ =peak rate factor (m<sup>3</sup>/s h/mm km<sup>2</sup>); and  $T_p$ =time to peak in h [Eq. (5)].

for paths that traverse long distances across the watershed as particles move downslope towards the outlet. The entire ensemble of particles is moved contemporaneously and the arrival times of individual particles at the watershed outlet are recorded. The cumulative arrival time distribution of the particle ensemble is the residence time distribution of excess rainfall on the watershed and contains information equivalent to an S-curve hydrograph. Alter-

natively, one could compute the total travel time along each path and rank order these arrival times to construct the arrival time distribution. By fitting a unit hydrograph model to this empirical S-curve, unit hydrograph parameters are recovered. Fig. 3 is one such cumulative arrival time distribution for the Ash Creek Watershed in Dallas, Tex.

The computational burden is extreme, even though the approach as presented is highly parallel (the particles do not interact). A purpose-built cluster computer (Cleveland and Smith

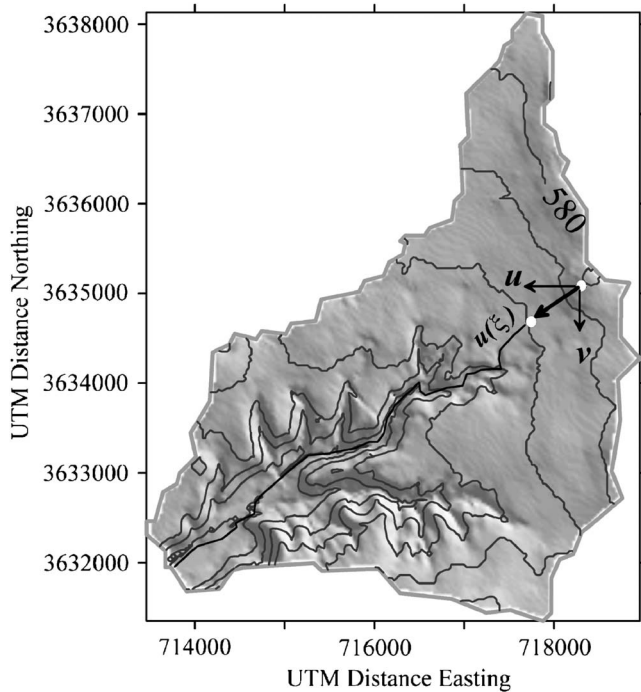


**Fig. 2.** Shaded relief map of watershed associated with USGS Gauging Station 08057320. Particle pathline, pathline, and Cartesian velocities are depicted for single runoff particle.

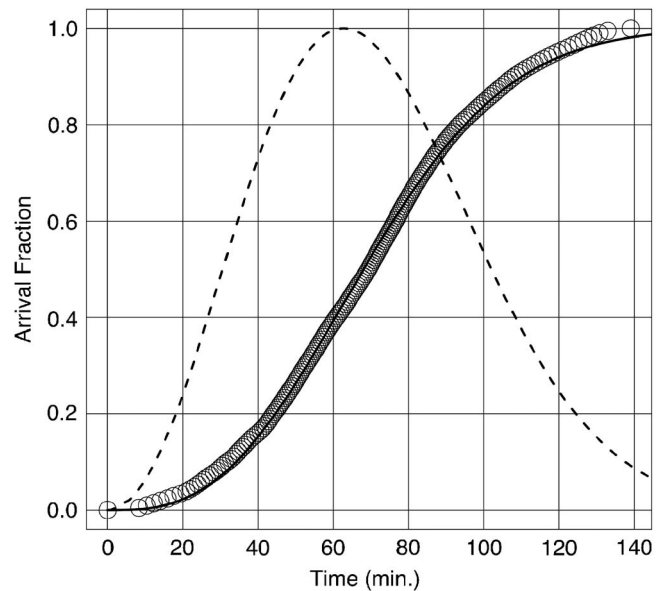


**Fig. 3.** Empirical cumulative arrival time distribution (open circles) and fitted cumulative unit hydrograph distribution (solid line). Cumulative unit hydrograph is integral of Eq. (4). Dashed line is dimensionless unit hydrograph for this watershed [Eq. (7)].

2004) was used to speed the computational throughput, by distributing the particle position computations among multiple processors. Despite taking advantage of the parallel structure of the problem, it still takes considerable time to complete the description of even a single watershed.

The unit hydrograph model selected for this research is a generalized gamma distribution (Leinhard 1964; Leinhard and Meyer 1967) and is expressed as

$$f(t) = \frac{\beta}{\Gamma(n/\beta)} \left(\frac{n}{\beta}\right)^{n/\beta} \frac{1}{t_{rm\beta}} \left(\frac{t}{t_{rm\beta}}\right)^{n-1} \exp\left[-\frac{n}{\beta} \left(\frac{t}{t_{rm\beta}}\right)^\beta\right] \quad (4)$$

The distribution parameters  $n$  and  $t_{rm\beta}$  have physical significance in that  $t_{rm\beta}$ =mean residence time of an excess raindrop on the watershed; and  $n$ =accessibility number, roughly proportional to the exponent on the distance-area relationship (a shape parameter);  $\beta$ =degree of the moment of the residence time;  $\beta=1$  would be an arithmetic mean, while for  $\beta=2$  the residence time is a root-mean-square time.  $\beta=2$  is used throughout this work, in part to be faithful to Leinhard's original derivation. Eq. (4) can also be expressed as a dimensionless hydrograph using the following transformations (Leinhard 1972) to express the distribution in conventional dimensionless form where  $Q_p$  and  $T_p$ =peak rate factor and time to peak of the hydrograph

$$t_{rm\beta} = \left(\frac{n}{n-1}\right)^{1/\beta} T_p \quad (5)$$

$$Q_p = f(T_p) \quad (6)$$

Expressed as a dimensionless hydrograph distribution Eq. (4) becomes

$$\frac{Q}{Q_p} = \left(\frac{t}{T_p}\right)^{n-1} \exp\left[-\frac{n-1}{\beta} \left(\left(\frac{t}{T_p}\right)^\beta - 1\right)\right] \quad (7)$$

The cumulative distribution function is determined by integrating Eq. (4) and this cumulative distribution is fit to the empirical S-curve hydrograph using a least square error minimization criterion. Once the distribution parameters  $n$  and  $t_{rm\beta}$  are recovered, they are then converted into conventional hydrograph parameters using Eqs. (5) and (6). Fig. 3 that shows the cumulative arrival time distribution for Ash Creek Watershed also displays the "fitted" Leinhard unit hydrograph, which is the source of the timing parameters for subsequent rainfall-runoff modeling.

The result is that the values of  $n$  and  $t_{rm\beta}$  are determined from a terrain model, which is conceptually equivalent to determining unit hydrograph parameters from physical watershed characteristics (for example, main channel length, slope, etc.), except this work considers the ensemble of characteristics (all the potential flow paths, all the slopes along these paths, etc.).

In addition to the generation of UH from the arrival time distribution a conventional analysis of the observed data to generate UH parameters was performed using the method described in Cleveland et al. (2006b).

## Application

The computer program that generated the arrival time distribution is referred to in this work as the digital terrain runoff model (DTRM). The DTRM was applied to the entire set of watersheds using 30-m digital elevation data. The watersheds were classified into "developed" and "undeveloped" watersheds. Representatives of each classification existed in all the database modules, thus the

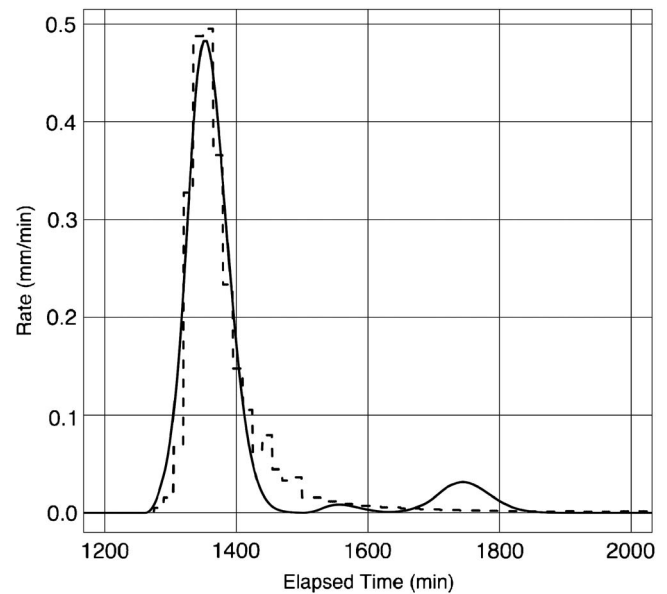


Fig. 4. Observed (dashed) and simulated (solid) runoff hydrograph for Ash Creek, May 27, 1975 storm

classification does not reflect a particular geographic location. The values used in Eq. (3) for generating the cumulative hydrographs for developed watersheds are  $n_f=0.04$  and  $d=0.2$ . These values were determined by trial and error using the Ash Creek Watershed, depicted in the Dallas area in Fig. 1. Ash Creek is a developed watershed with drainage area of 18.6 km<sup>2</sup>, a dimensionless slope of 0.006, and a main channel length of 8.7 km. The June 3, 1973 storm was used to calibrate the particle-tracking model. These two values were applied to all developed watersheds regardless of size and location.

The values used in Eq. (3) for generating the cumulative hydrographs for undeveloped watersheds are  $n_f=0.08$  and  $d=0.2$ , and were determined by a similar single-storm trial and error "calibration" of the Little Elm Watershed, slightly northwest of Dallas, also depicted in Fig. 1. Little Elm is an undeveloped watershed with drainage area of 189.5 km<sup>2</sup>, a dimensionless slope of 0.0024, and a main channel length of 37.4 km. These two values were applied to all undeveloped watersheds regardless of size and location.

For each watershed, DTRM was run once using the appropriate  $n_f$  and  $d$  values and a single Leinhard hydrograph, with two parameters,  $n$  and  $t_{rm\beta}$ , is generated for each watershed. These two values are determined entirely from topographic data and the assumed  $n_f$  and  $d$ ; no actual rainfall-runoff data are used by the DTRM.

To evaluate the performance of the estimation procedure, historical rainfall data are applied to the watershed and the runoff is simulated. These simulated runoff hydrographs are compared to observed runoff hydrographs. Fig. 4 is a representative example of output from this testing using observed data from the writers' database. The observed hydrograph is the dashed line with the stepwise changes in value, while the smooth curve is the model result using the same hyetograph (input rainfall) and convolving this rainfall with the Leinhard unit hydrograph using the watershed values for  $n$  and  $t_{rm\beta}$ . The plot in Fig. 4 is typical, but not all storms were reproduced equally well.

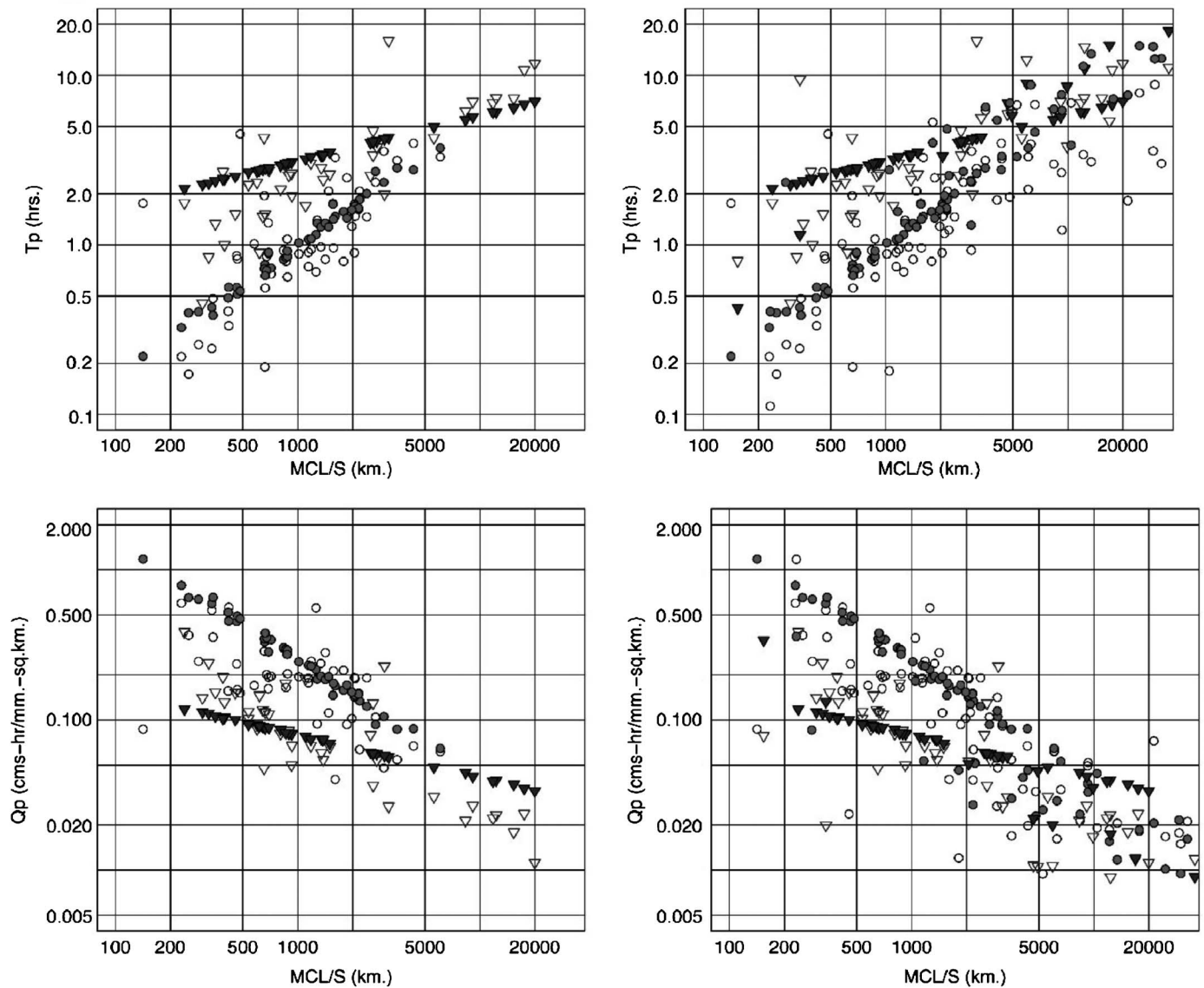


**Fig. 5.** Relationship of  $T_p$  and  $Q_p$  for Texas watersheds. MCL/S is ratio of main channel length to slope. Left panels exclude Houston watersheds. Right panels include Houston watersheds: (○)=station median values of conventional parameters for developed watersheds; (▽)=station median values of conventional parameters for undeveloped watersheds; (●)=station values of DTRM-derived parameters for developed watersheds; and (▼)=station values of DTRM-derived parameters for undeveloped watersheds.

## Results and Discussion

Fig. 5 is a set of plots that illustrate the unit hydrograph parameters estimated using the DTRM procedure and by conventional analysis. The conventional analysis produces a different pair of  $Q_p$  and  $T_p$  for each storm, and median of these values is compiled and reported for each station, while the DTRM model only produces a single pair of  $Q_p$  and  $T_p$  for each station. The conventional-derived values are shown in Fig. 5 as open markers. The DTRM-derived values are plotted as closed markers. The two left panels present the results for the Central Texas watersheds (excluded Houston) and the right panels present the results for all the study watersheds. The horizontal axis is the ratio of main channel length to slope. This particular explanatory variable was chosen as a way to represent different watershed sizes and slopes on a single plot.

In right hand panels (includes Houston), there is an increase in variability attributed to the Houston watersheds. As mentioned

earlier, the Houston watersheds not only have low slope, but backwater effects are known to be significant and contribute the variability in both the  $T_p$  and  $Q_p$  plots. If the Houston data are removed from the plots, the variability is reduced, as in the left hand panels.

Hypothesis tests that the median  $T_p$  and  $Q_p$  values estimated by either procedure, when classified by watershed development, showed that there was no evidence to reject the null hypothesis that the median values are the same for either method of estimation at a level of significance of  $\alpha=0.05$ . Fig. 5 and the statistical tests support a conclusion that the DTRM model generates unit hydrographs that are comparable to hydrographs generated by conventional analysis of rainfall-runoff data.

Fig. 6 is a set of plots that qualitatively illustrate the performance of the approach on over 2,600 storms. The left panels are the results when the unit hydrographs are generated using the DTRM procedure and the right panels are the same storms, except that the hydrograph parameters were determined by conventional



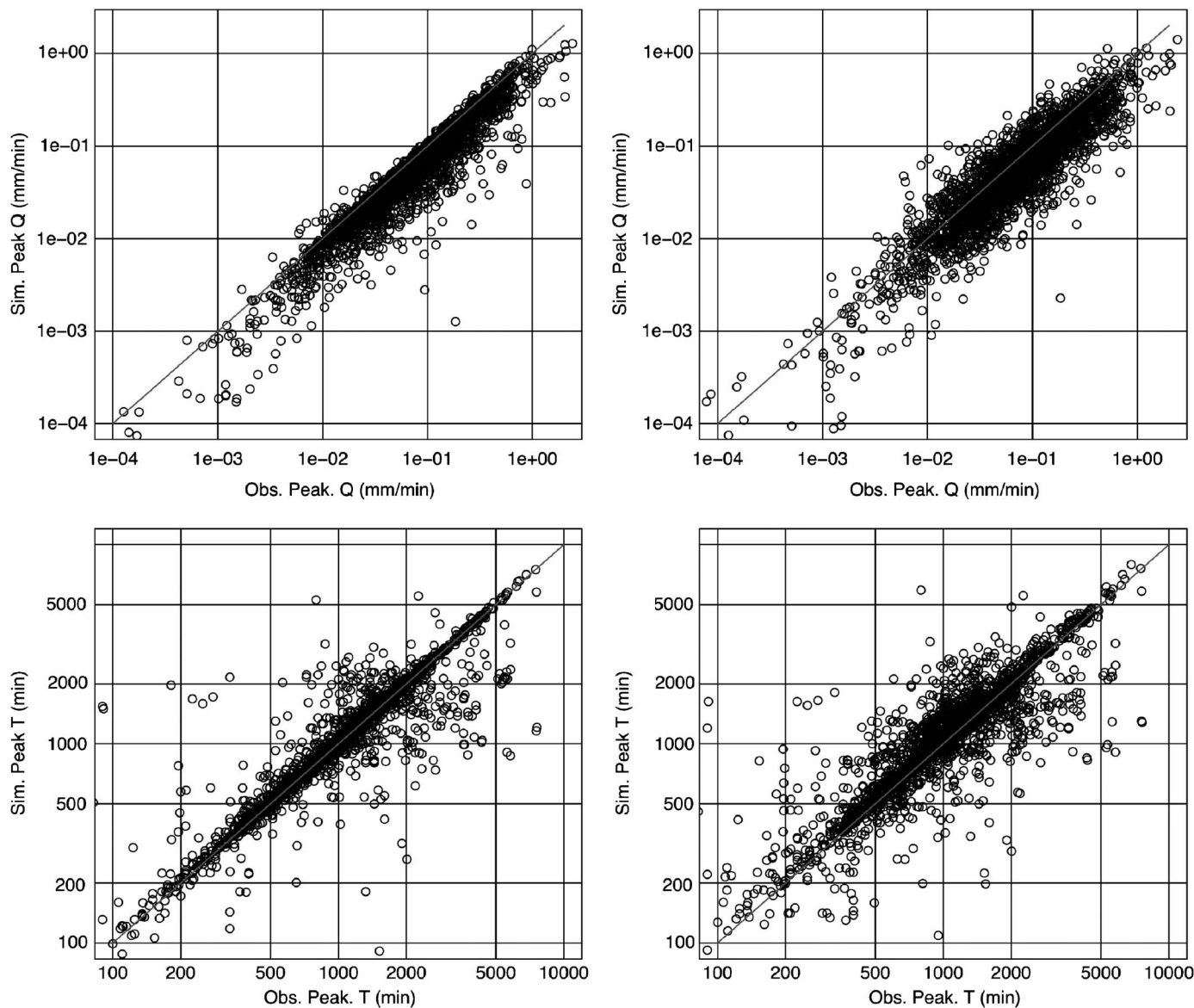


**Fig. 6.** Relationship of simulated and observed peak flows ( $Q$ ) and time of peak flows ( $T$ ) for storms using conventional hydrograph analysis (left images) and particle tracking model (right images)

analysis (i.e., rainfall and runoff data are used, no knowledge of watershed physical characteristics is used). The upper plots are the observed peak discharge and simulated peak discharge for individual storms. An equal-value line is plotted that represents an ideal result. The variability of the DTRM procedure is larger, and the DTRM result is more symmetric around the equal value line. The increased variability is anticipated as the method has no access to rainfall data to estimate hydrologic response.

The lower plots are the time when the peak discharge occurred in either the observations or the simulations. As in the upper plots, the variability for the DTRM procedure is larger. The median values of the peak discharge or time of peak discharge (for roughly 2,600 storms) are similar regardless of classification (observed, simulated DTRM, simulated conventional). A Kruskal–Wallis test supports this conclusion—there is no evidence to reject the null hypothesis that the median values do not differ for either method when compared to each other or to the observations at a level of significance of  $\alpha=0.05$ .

The watersheds were classified as undeveloped and developed.

The rainfall and runoff observations across these two classifications were also analyzed to determine if there was a difference between classifications, either for rainfall or runoff.

The median and interquartile range for rainfall depth are nearly the same for either classification. A rank-sum test for difference in the median values shows that there is insufficient evidence to reject the null hypothesis that the difference in median values of rainfall depth for these two classifications is zero at a level of significance of  $\alpha=0.05$ . Thus the rainfall depths are the same regardless of whether a watershed is developed or undeveloped.

The median and interquartile range for runoff depth are lower and narrower for the undeveloped watersheds as compared to the developed watersheds. The outlier portions of both classifications have similar patterns. A rank-sum test for difference in the median values shows that there is sufficient evidence to reject the null hypothesis that the difference in median values of runoff depth for these two classifications is zero at a level of significance of  $\alpha=0.05$ . Thus the runoff produced by a developed watershed is

different from an undeveloped watershed, and developed watersheds appear to convert more rainfall to runoff than an undeveloped watershed (by a factor of roughly two).

An additional set of comparative results is reported in Cleveland et al. (2006a) where the time to accumulate 98% of the unit hydrograph area ( $T_{98}$ ) was used as a surrogate for the time of concentration ( $T_c$ ). These  $T_{98}$  values compared favorably to  $T_c$  determined by several methods reported in Roussel et al. (2005).

## Conclusions

The conclusions of this study are that the DTRM procedure is a reasonable approach to estimate UH parameters from a relatively minimal description of watershed properties—in this case elevation and a classification of developed or undeveloped. The elevation data are available on the Internet, or can be prepared from paper-based maps. The classification as to developed or undeveloped can be made based on aerial imagery. The method produced UH comparable to those determined by conventional analysis and thus is a useful synthetic hydrograph approach.

Based on the review of prior work, the procedure is similar to GUH approaches, but simpler in that it disregards stream order, bifurcation rules, channel flow, and other measures. The procedure is also similar to existing GIS methods except instead of routing flows along a path, the travel time along a path is used to generate an arrival time distribution.

The runoff volumes are statistically different from developed watersheds as compared to undeveloped watersheds, and the difference is evident in the conventional results. No attempt was made to optimize the unit velocity terms in Eq. (3) to account for different land uses, etc., yet the approach simulated episodic behavior at about the same order of magnitude as observed behavior in terms of peak discharge and timing. The writers speculate that some variability might be reduced by such an exercise but it would greatly complicate the process.

The results in Fig. 5 suggest that a lower bound of slope somewhere between 0.0002 and 0.002 exists below which kinematic-wave type equations should not be used without careful consideration.

## Acknowledgments

The writers would like to acknowledge the support of the Texas Department of Transportation, program coordinator David Stolpa, P.E., project directors Jaime Villena-Morales, P.E., and George R. Herrmann, P.E. The writers also acknowledge contributions from their colleagues, Dr. William Asquith, Meghan Roussel, and Amanda Garcia at the U.S. Geological Survey, Austin, Texas. This study was supported through Texas Department of Transportation research Project Nos. 0-4193, 0-4194, and 0-4696. The contents of this paper reflect the views of the writers. The contents do not reflect the official view or policies of the Texas Department of Transportation (TxDOT). This paper does not constitute a standard, specification, or regulation.

## References

Asquith, W. H., Thompson, D. B., Cleveland, T. G., and Fang, X. (2004). "Synthesis of rainfall and runoff data used for Texas Department of

- Transportation Research Projects 0-4193 and 0-4194." *U.S. Geological Survey Open-File Rep. No. 2004-1035*, Center, Miss.
- Clark, C. O. (1945). "Storage and the unit hydrograph." *Trans. Am. Soc. Civ. Eng.*, 110, 1419-1446.
- Cleveland, T. G., Fang, X., and Thompson, D. B. (2006a). "Timing parameter estimation using a particle tracking method." *Texas Department of Transportation Research Rep. No. 0-4696-3*, Austin, Tex.
- Cleveland, T. G., He, X., Asquith, W. H., Fang, X., and Thompson, D. B. (2006b). "Instantaneous unit hydrograph selection for rainfall-runoff modeling of small watersheds in North and South Central Texas." *J. Irrig. Drain. Eng.*, 132(5), 479-485.
- Cleveland, T. G., and Smith, M. T. (2004). "Darkstar cluster computer." (<http://cleveland1.cive.uh.edu/computing/darkstar/index.html>) (Nov. 16, 2006).
- Gupta, V. K., Waymire, E., and Wang, C. T. (1980). "A representation of an instantaneous unit hydrograph from geomorphology." *Water Resour. Res.*, 16(5), 855-862.
- Hydrologic Engineering Center (HEC). (2000). "Hydrologic modeling system HEC-HMS." *Technical reference manual*, U.S. Army Corps of Engineers, Davis, Calif.
- Jin, C. (1992). "A deterministic gamma-type geomorphologic instantaneous unit hydrograph based on path types." *Water Resour. Res.*, 28(2), 479-486.
- Kull, D. W., and Feldman, A. D. (1998). "Evolution of Clarks unit graph method to spatially distributed runoff." *J. Hydrol. Eng.*, 3(1), 9-19.
- Lee, K. T., and Yen, B. C. (1997). "Hydrograph derivation." *J. Hydraul. Eng.*, 123(1), 73-80.
- Leinhard, J. H. (1964). "A statistical mechanical prediction of the dimensionless unit hydrograph." *J. Geophys. Res.*, 69(24), 5231-5238.
- Leinhard, J. H. (1972). "Prediction of the dimensionless unit hydrograph." *Nord. Hydrol.*, 3, 107-109.
- Leinhard, J. H., and Meyer, P. L. (1967). "A physical basis for the generalized gamma distribution." *Q. Appl. Math.*, 25(3), 330-334.
- Maidment, D. R. (1993). "Developing a spatially distributed unit hydrograph by using GIS." *Proc. of the Vienna Conf., HydroGIS93*, IAHS Pub. No. 211, 181-192.
- Muzik, I. (1996). "Lumped modeling and GIS in flood predictions." *Geographical information systems in hydrology*, V. P. Singh, ed., Kluwer Academic, Dordrecht, The Netherlands.
- O'Calligan, J. F., and Mark, D. M. (1984). "Extraction of drainage networks from digital elevation data." *Comput. Vis. Graph. Image Process.*, 28, 323-344.
- Olivera, F., and Maidment, D. (1999). "Geographic information systems (GIS)-based spatially distributed model for runoff routing." *Water Resour. Res.*, 35(4), 1135-1164.
- Rodriguez-Iturbe, I., and Valdes, J. B. (1979). "The geomorphologic structure of hydrologic response." *Water Resour. Res.*, 15(6), 1409-1420.
- Roussel, M. C., Thompson, D. B., Fang, X., Cleveland, T. G., and Garcia, A. C. (2005). "Timing parameter estimation for applicable Texas watersheds." *Texas Department of Transportation Research Rep. No. 0-4696-2*, Austin, Tex.
- Saghafian, B., and Julien, P. Y. (1995). "Time to equilibrium for spatially variable watersheds." *J. Hydrol.*, 172, 231-245.
- Saghafian, B., Julien, P. Y., and Rajaie, H. (2002). "Runoff hydrograph simulation based on time variable isochrone technique." *J. Hydrol.*, 261, 193-203.
- Shamseldin, A. Y., and Nash, J. E. (1998). "The geomorphological unit hydrograph—A critical review." *Hydrology Earth Syst. Sci.*, 2(1), 1-8.
- Sherman, L. K. (1932). "Stream flow from rainfall by the unit-graph method." *Eng. News-Rec.*, 108, 501-505.
- Wooding, R. A. (1965). "A hydraulic model for the catchment-stream problem." *J. Hydrol.*, 3, 254-267.